GENERAL RESEARCH

Integrated Modeling and Simulation for Improved Reactive Drying of Clearcoat

H. H. Lou and Y. L. Huang*

Department of Chemical Engineering and Materials Science, Wayne State University, Detroit, Michigan 48202

Clearcoat filmbuild is one of the main concerns for painting quality in automotive paint shops. In operation, clearcoat is sprayed on the vehicle surface and then baked in an oven where solvents are removed and cross-linking reactions take place. Because of operational complexity and measurement difficulty, the process dynamics is basically unknown. Thus, the operational settings in the oven are solely experience-based. Hitherto, the studies on automotive oven operations has been only at the lab level. To significantly improve clearcoat filmbuild, a model at the plant floor level should be developed. In the present work, a first-principles-based, simplified, integrated dynamic model is developed to characterize the clearcoat reactive drying process in an oven. It is demonstrated that the model can provide satisfactory long-term predictions of filmbuild, facilitate a thorough analysis of drying/curing operations, and form the basis for developing optimal operational strategies for improving film quality and reducing defects.

Introduction

Automotive coating involves paint applications of several thin layers, such as phosphate, electrocoat, powder, basecoat, and clearcoat. The thickness and uniformity of the clearcoat have utmost importance for the appearance and durability of vehicle coatings.[1] In practice, however, the in-specification rate of clearcoat film thickness of vehicles is typically less than 30% in paint shops. The film uniformity is rather poor, especially for the vertical panels of vehicles. The filmbuild problems, together with others, have caused the generation of a variety of defects, such as orange peels, craters, blisters, runs, sags, and fish eyes, on the vehicle surface; many of them are due to improper oven operation.[2]

In an oven, the solvents contained in the film are dried off as the vehicle panels are heated. The film thickness is then reduced, and cross-linking reactions take place. In operation, various uncertainties exist because of process complexity and measurement difficulty.[3] Thus, it is still unknown what the optimal panel heating pattern in each zone should be and how a drying pattern should be set to minimize defects and maximize the production rate. It is still unclear how a cross-linking reaction progresses in an oven. There is even less knowledge about the wet film thickness and uniformity on panels when a vehicle enters the oven. Under these circumstances, it is certainly extremely difficult to ensure coating quality. In plants, the coating quality is under open-loop control because no single piece of coating information is used for oven feedback control. To eventually realize closed-loop quality control, two kinds of efforts must be made: (i) to obtain sufficient real-time process information and (ii) to predict precisely the process dynamics and then to optimize process operation. The first effort is largely dependent upon the availability of low-cost, nondestructive, and reliable sensors. There is no quick solution now. The second effort is probably more essential. The fundamental component for process prediction and optimization is process dynamic modeling.

Model-based quality control is consistent with the concept of so-called next generation quality control (NGQC) that was introduced by Wu et al.[4] The focal point of the concept is to prevent the generation of quality problems through process modeling and real-time optimization. This is fundamentally different from traditional inspection-based QC approaches that are reactive to quality problems. A NGQC approach must be proactive to quality problems, which means that it must be prevention-oriented, aiming at the elimination of quality problems from the beginning.

Automotive reactive drying is one of the most critical, yet most complex, processes in the automotive coating industry. Over the past years, vigorous attempts have been made to model the oven drying process. Blanc et al. developed a model for coupled material transformations with heat- and mass-transfer phenomena that occur during the convective or infrared drying of coated films of model car painting.[5] Dickie et al. modeled a curing process and evaluated curing strategies based on the chemical understanding of polymerization processes and basic heat-transfer principles.[6] The model developed by Howison et al. described the influence of the surface tension, viscosity, solvent diffusivity, and solvent evaporation rate in different coating layers.[7] The studies have provided better understanding of the paint drying/curing operations. These models, however, are basically at the lab level. They are highly nonlinear and

* To whom correspondence should be addressed. Phone: 313-577-3771. Fax: 313-577-3810. E-mail: yhuang@chem1.eng.wayne.edu.

10.1021/ie990171g CCC: $19.00
Published on Web 01/22/2000

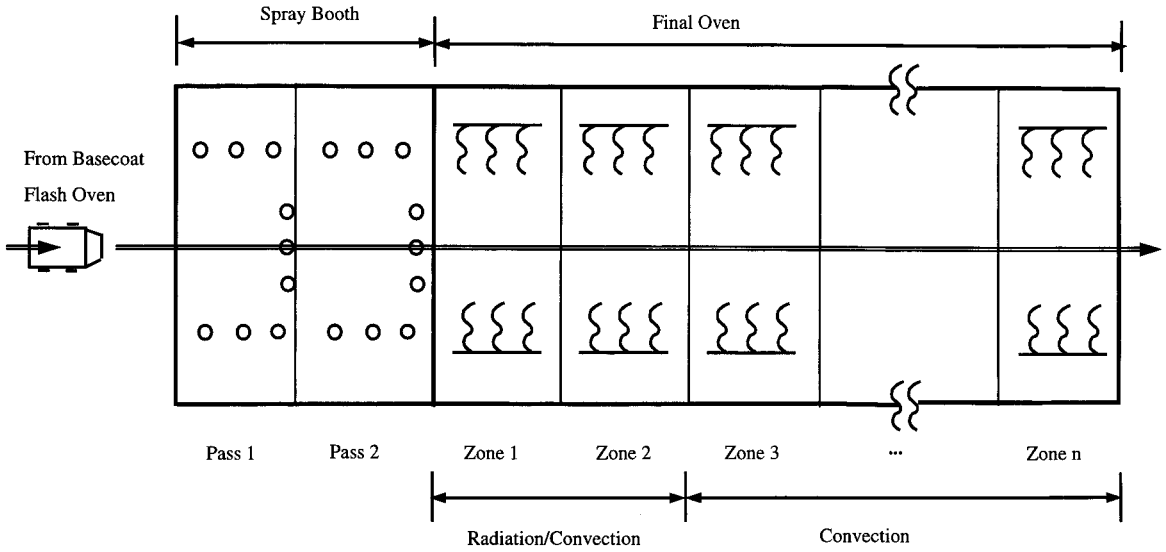

Figure 1. Flow chart of a typical clearcoat spray and oven-baking process.

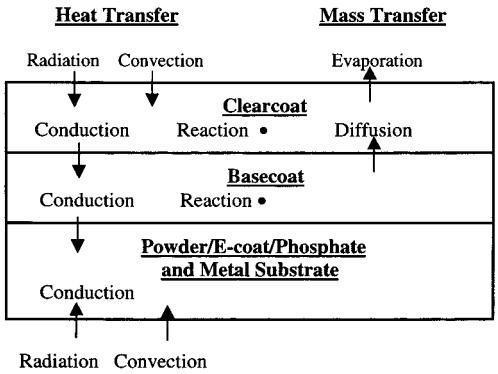

Figure 2. Heat- and mass-transfer and reaction mechanisms in different layers of coatings on vehicle panels.

too rigorous. There must be considerable model mismatch and computational difficulties for on-line real applications.

In the present paper, we introduce a first-principle-based, simplified, integrated plant floor dynamic model for characterizing the reactive drying of clearcoat in an oven. Model-based simulation will show simultaneously how the film is dried and how the cross-linking reaction takes place under different operating conditions and with different wet film thicknesses. Initial success in filmbuild improvement through adjusting process parameters will also be demonstrated. The potential of model-based optimization will also be discussed.

Clearcoat Application Process

A typical clearcoat spray and curing process is illustrated in Figure 1. Vehicle bodies on the conveyor move through the process at a constant line speed. In the spray booth, the spray bells deliver paint droplets onto each vehicle panel to generate a wet film. Vehicles then enter the final oven for baking. A spray booth may have several passes of spraying, while a final oven is divided into a number of zones with different heating mechanisms.[8]

In an oven, three types of interdependent phenomena occur. As depicted in Figure 2, they are (i) the heat transfer on vehicle panels due to radiation, convection, and conduction, (ii) the mass transfer of solvents through diffusion and evaporation that leads to the changes of moisture content and film thickness, and (iii) the cross-linking reaction that causes the film-forming chemicals in paint to flow together and form a three-dimensional (3-D) molecular network. This is a reactive drying process where physical drying and chemical polymerization take place simultaneously. Chemical reactions occur with phase changes, such as gelation and vitrification. Operational modes directly influence the physical, chemical, and mechanical properties of the final coating. Improper operation can lead to the generation of various defects. As observed, a very high drying speed causes fast solvent removal and then probably defects such as popping and orange peels. An overbaking situation will deteriorate the physical properties of the film, such as adhesion and coating strength. The formation of blisters, crinkling, and bubbling is another example. These defects are all caused by the exposure of the film in a high-temperature environment for an improperly long time. On one hand, if the temperature exceeds the solvent boiling point, bubbles can form. When they burst, blisters will form. Crinkling is also caused by the bubbles that pucker the surface. If the temperature is too high, it can even raise the skin up. On the other hand, if the temperature is too low, a cross-linking reaction can never be accomplished.

Needless to say, to have a deep understanding of the fundamentals of drying and polymerization operations is the first, necessary step toward a substantial improvement of clearcoat filmbuild. In this regard, the development of an oven process model becomes a must.

Modeling

A mathematical model for reactive drying in an oven should be an integrated one that characterizes both physical drying and the chemical reaction occurring in the clearcoat. More specifically, the model needs to provide the following dynamics information on the clearcoat: (i) panel heating, (ii) solvent removal, (iii) cross-linking reaction, and (iv) film thickness changes.

Major Assumptions and Process Variables. To facilitate the modeling, the following major assumptions are made in this work:

(a) The temperature of each panel is uniformed in any zone of an oven. This means that no temperature gradient exists in the film and metal substrate. The

assumption can be justified by evaluating the Biot number (Bi) which is the ratio of l/k over $1/h_T$, where l/k represents the internal resistance to heat transfer by conduction and h_T is the coefficient of total heat transfer by conduction, convection, and radiation between the surroundings and the panel surface.[9] In a convection zone, convection is the dominating factor. Thus, h_T is approximately equal to h_v. In the radiation/convection zone, radiation heat is also considerable. Thus, h_T is the sum of h_v and h_r. For a very thin layer (10−50 μm), the coating surface absorbs only a fraction of the incident radiation and transmits the rest to the inner side. Hence, the temperature of a coating layer can be considered uniformed. This has been proven by industrial applications. For a typical polymer coating, thermal conductivity k is about 0.2 W/m·K and the thickness of the coating, l, is about 10−50 μm. For a typical baking process, the heat-transfer coefficient h_T is around 5−50 W/m^2·K. This gives a very small Bi ($\leq$0.025) value.

(b) The solvent residue in the basecoat is negligible when a vehicle moves into the oven. In fact, the solvent in the basecoat has been nearly completely evaporated in the flash oven before clearcoat spray begins. Thus, no solvent diffusion from the basecoat to the clearcoat should be considered in modeling.

(c) The thickness change of the film from wet to dry is dominated by the removal of solvents in paint. The film shrinkage (or expansion, according to some literature) due to a cross-linking reaction in an oven is no more than 3% for the paint considered. This indicates that the reaction-related film volume change can be safely ignored.

(d) The paint density of clearcoat (ρ_c) changes as the solvent is removed. In this work, the clearcoat density is approximated as

$$\rho_c = \frac{V_s\rho_s + V_l\rho_l}{V_s + V_l} \tag{1}$$

where ρ_l and ρ_s are, respectively, the densities of the reducible component (e.g., solvent) and unreducible components (solids, additives, etc.) in paint; V_l and V_s are the corresponding volumes. As an example, the wet film may contain 30% of solvent in volume. Thus, the ratio of the density for a wet film to that for dry film is at least 0.7.

(e) The heat caused by the polymerization reaction and solvent evaporation is negligible, when it is compared with radiation and convection heat. Heat loss from the oven wall is assumed to be negligible.

(f) The heat and mass transfer along the film surface is neglected because the film is extremely thin ($\leq$50 μm), as compared with the surface area (>0.5 × 1 m^2). The adoption of this assumption can greatly accelerate computations without any significant errors. Certainly, any rigorous modeling should consider the three-dimensional effect and a ray tracing method needs to be employed to explain the different rates of radiative heat transfer on the various surfaces.

With these assumptions, three classes of process variables are identified for modeling: (i) manipulated variables (oven wall temperatures, convection air temperatures, and velocities in different zones), (ii) controlled variables (panel temperatures, clearcoat film thickness, drying rates, and reaction conversion rates), and (iii) disturbance variable (wet film thickness, line speed, and panel initial temperatures). Using basic mass- and heat-transfer principles, polymerization kinetics, and modern control theories, we can develop an integrated dynamic model.

Panel Heating Model. An oven usually over 100-m long is divided into a number of zones where heating mechanisms and operational settings are different. In the oven, the first two zones have mainly radiation with high-energy flux but with no or very low air flow to avoid contamination by dust on the wet film. Convection air in the succeeding zones increases the heat- and mass-transfer coefficients at the same time. The last zone is always relatively cool, which provides residence time for coating to equilibrate with ambient air and to continue the polymerization reaction. A general energy equation is

$$\rho_m C_{p_m} Z_m \frac{dT}{dt} = \mathcal{T}\sigma\epsilon(T_w^4 - T^4) + h_v(T_a - T) \tag{2}$$

where $\rho_m C_{p_m} Z_m$ is for the metal substrate. Rigorously, the left-hand side of the equation should include the terms for all other coating layers. However, the coatings are so thin that the rate of change of heat in them has no comparison in magnitude with that for the substrate.

For the zones with only convection, the radiation term in eq 2 was dropped. The model becomes

$$\rho_m C_{p_m} Z_m \frac{dT}{dt} = h_v(T_a - T) \tag{3}$$

The heat-transfer coefficient, h_v, is a function of convection air velocity (V_a), the distance between the panel and the convection air nozzles, and others (expressed by β). According to Cohen and Gutoff, it can be expressed as[1]

$$h_v = \beta V_a^{0.7} \tag{4}$$

Clearcoat Drying Model. As depicted in Figure 2, a drying model should characterize the solvent evaporation process on the film surface and the diffusion process within the film. To facilitate the modeling, we can divide the clearcoat film into a number of very thin slices, each of which has a fixed thickness (ΔZ). If the initial thickness of the clearcoat is Z_0, the total number of slices will be

$$N_0 = \text{int}\left(\frac{Z_0}{\Delta Z}\right) \tag{5}$$

The slices are numbered starting from the one just above the basecoat surface. There is no mass transfer from the basecoat to the first slice of clearcoat because it is assumed that the basecoat is dry already when entering the oven. The mass change in the slice is equal to the solvent diffusion from the first slice to the second, that is,

$$\Delta Z \frac{\partial X}{\partial t} = D(X,T)\frac{\partial X}{\partial Z} \tag{6}$$

Note that the diffusivity, $D(X,T)$, is dependent on the film temperature and solvent content. It can be expressed as

$$D(X,T) = \eta e^{-((\gamma/X)+(E_d/RT))} \tag{7}$$

where η is a pre-exponential constant for diffusion, γ a constant, and E_d the activation energy for diffusion.[10]

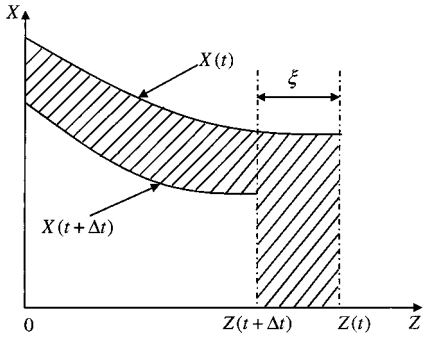

Figure 3. Illustration of the film shrinkage due to moisture change.

For any slice (ith) from the second to the ($N - 1$)th, the change of solvent content is caused by the diffusion from the ($i - 1$)th to it and that from it to the ($i + 1$)th. This relationship can be expressed as

$$\frac{\partial X}{\partial t} = \frac{\partial}{\partial Z}\left(D(X,T)\,\frac{\partial X}{\partial Z}\right) \tag{8}$$

For the top slice (i.e., the Nth), the drying rate, R_{dry}, defined as the change of mean solvent loss over the time ($-\mathrm{d}\bar{X}/\mathrm{d}t$), is controlled by solvent evaporation to the surroundings. The evaporation is largely determined by the solvent partial pressure as well as the mass-transfer coefficient (K). This relationship can be described as

$$\rho_s Z_s\,\frac{\partial X}{\partial t} = K\frac{(P_a - \alpha P_{sa})}{P} + \rho_s D(X,T)\,\frac{\partial X}{\partial Z} \tag{9}$$

where Z_s is the thickness of unreducible components in the film.

Film Thickness Model. The film thickness changes are mainly due to solvent removal. Rigorously, the moisture contents on a panel surface vary in locations so that it is desirable to use a quadrate term to describe the film shrinkage. Practically, however, this difference in moisture contents is much less than that along the film thicknesses. Assume at time t, the film thickness and film solvent content are $Z(t)$ and $X(t)$, respectively. After a sampling time interval Δt, the film thickness and solvent content are reduced to $Z(t + \Delta t)$ and $X(t + \Delta t)$, respectively. The film thickness reduction in this time interval is ξ, as depicted in Figure 3. The solvent content varies nonlinearly along the film thickness. The amount of solvent removed in a time interval can be formulated below:

$$\rho_l \xi = \rho_s\left(\int_0^{Z(t)} X(t)\,\mathrm{d}Z - \int_0^{Z(t+\Delta t)} X(t+\Delta t)\,\mathrm{d}Z\right) \tag{10}$$

where ρ_l and ρ_s are the densities of the solvent and unreducible components in paint, respectively. In this formula, the first and the second terms on the right-hand side represent, respectively, the total moisture contents in the film at the time t and $t + \Delta t$, if each term is multiplied by the surface area of a panel. The difference of the two terms is the total amount of moisture removed from the whole panel during the period, Δt. Because it undergoes no change during drying, the film surface area does not appear in eq 10.

Polymerization Model. The cross-linking reaction during the curing operation is rather complicated. The reaction conversion rate is determined by paint properties and film temperature that changes dynamically. It is found that a first-order reaction can characterize the main feature of the cross-linking reaction and quantify the effects of modest variable changes in a cure cycle in the oven.[6] On the basis of this observation, the following simplified model is adopted here,

$$\frac{\mathrm{d}x}{\mathrm{d}t} = \kappa(1 - x) \tag{11}$$

$$\kappa = \zeta \mathrm{e}^{-E_r/RT} \tag{12}$$

where x is the polymerization conversion rate, κ the polymerization reaction constant, E_r the reaction activation energy, and ζ the reaction frequency factor.

State-Space Model

For real-time control, the differential and integral models described in the preceding section need to be discretized. This will result in a set of state-space models. In derivation, a piecewise linearization approach was adopted.[11,12] This approach has been extensively used to linearize PDEs at the nominal operating point in numerous industrial applications.

As each vehicle moves into a new zone of an oven successively, the heating mechanisms and operational parameter settings will be changed. To use the model properly, the time at which the boundary condition changes must be identified. The time intervals (J_i) required for a vehicle to pass the ith zone can be calculated on the basis of the conveyor line speed, s, and the length of the zone, L_i, that is,

$$J_i = \frac{L_i}{s\Delta t} \tag{13}$$

Discrete Panel Heating Model. The heating model in eqs 2 and 3 can be readily discretized below,

$$T(j+1) = aT(j) + b_1 T_w(j) + b_2 T_a(j) \tag{14}$$

where

$$a = \begin{cases} 1 - [(4\mathscr{T}\sigma\epsilon T(j-1)^3 + h)\Delta t]/\rho_m C_{p_m} Z_m; \\ \qquad \text{(a) radiation and convection} \\ 1 - h\Delta t/\rho_m C_{p_m} Z_m; \\ \qquad \text{(b) convection only} \end{cases} \tag{15}$$

$$b_1 = \begin{cases} [4\mathscr{T}\sigma\epsilon T_w(j-1)^3\Delta t]/\rho_m C_{p_m} Z_m; \\ \qquad \text{(a) radiation and convection} \\ 0; \qquad \text{(b) convection only} \end{cases} \tag{16}$$

$$b_2 = \frac{h\Delta t}{\rho_m C_{p_m} Z_m} \tag{17}$$

As indicated, coefficients a and b_1 in eqs 15a and 16a are for the radiation/convection zones and those in eqs 15b and 16b are for the convection-only zones.

Discrete Drying Model. In discretizing eqs 6−9, the following finite difference relationships are used for the partial differential terms:

$$\frac{\partial X}{\partial Z} = \frac{X_n(j+1) - X_n(j)}{\Delta Z} \tag{18}$$

$$\frac{\partial}{\partial Z}\left(D(X,T)\frac{\partial X}{\partial Z}\right) = \left(\frac{D_{n+1}(j) - D_n(j)}{\Delta Z}\right)\left(\frac{X_{n+1}(j) - X_n(j)}{\Delta Z}\right) + D_n(j)\left(\frac{X_{n+1}(j) - 2X_n(j) + X_{n-1}(j)}{\Delta Z^2}\right) \quad (19)$$

Using these expressions, we have the following linear model.

$$\mathbf{X}(j+1) = \mathbf{A}\mathbf{X}(j) + \mathbf{B}\mathbf{U}(j) \quad (20)$$

where

$$\mathbf{X}(j) = (X_1(j) \quad X_1(j) \quad \dots \quad X_{N-1}(j) \quad X_N(j))^{\mathrm{T}} \quad (21)$$

$$U(j) = \frac{1}{P} \quad (22)$$

$$\mathbf{A} = \begin{pmatrix} a_{1,1} & a_{1,2} & & & \\ a_{2,1} & a_{2,2} & a_{2,3} & & \\ & \ddots & \ddots & \ddots & \\ & a_{N-1,N-2} & a_{N-1,N-1} & a_{N-1,N} & \\ & & a_{N,N-1} & a_{N,N} & \end{pmatrix} \quad (23)$$

$$\mathbf{B} = (0 \quad 0 \quad \dots \quad 0 \quad b_N)^{\mathrm{T}} \quad (24)$$

where

$$a_{1,1} = 1 + \frac{D_1(j)\Delta t}{\Delta Z^2} \quad (25)$$

$$a_{1,2} = 1 - a_{1,1} \quad (26)$$

$$a_{n,n-1} = \frac{D_n(j)\Delta t}{\Delta Z^2}, \qquad n = 2, 3, \dots, (N-1) \quad (27)$$

$$a_{n,n+1} = \frac{D_{n+1}(j)\Delta t}{\Delta Z^2}, \qquad n = 2, 3, \dots, (N-1) \quad (28)$$

$$a_{n,n} = 1 - a_{n,n-1} - a_{n,n+1}, \qquad n = 2, 3, \dots, (N-1) \quad (29)$$

$$a_{N,N-1} = -\frac{\Delta t D_N(j)}{\Delta Z^2} \quad (30)$$

$$a_{N,N} = 1 - a_{N,N-1} \quad (31)$$

$$b_N = \frac{K(P_{\mathrm{a}} - aP_{\mathrm{sa}})\Delta t}{\rho_{\mathrm{s}}\Delta Z} \quad (32)$$

In determining these coefficients, diffusivity $D(X,T)$ in eq 7 should also be discretized in the following form:

$$D_n(j) = \eta \mathrm{e}^{-[\gamma/X_n(j) + E_{\mathrm{d}}/RT(j)]}; \qquad n = 1, 2, \dots, N \quad (33)$$

Discrete Film Thickness Model. The film thickness model in eq 10 is an integral equation. In discretization, the integral term can be expressed as follows.

$$\int_0^{Z(t)} f(t)\,\mathrm{d}Z = \sum_{n=1}^{\mathrm{int}[Z(j)/\Delta Z]} f_n(j)\Delta Z \quad (34)$$

The final form of the model becomes

$$Z(j+1) = Z(j) - \left(\frac{\rho_{\mathrm{s}}\Delta z}{\rho_{\mathrm{l}} - \rho_{\mathrm{s}}X_n(j+1)}\right) \sum_{n=1}^{\mathrm{int}(Z(j)/\Delta Z)} (X_n(j) - X_n(j+1)) \quad (35)$$

Discrete Polymerization Model. The kinetic model in eqs 11 and 12 can be readily derived as follows,

$$x(j+1) = ax(j) + bT(j) \quad (36)$$

where

$$a = 1 - \zeta\Delta t \mathrm{e}^{-[E_{\mathrm{r}}/(RT(j-1))]} \quad (37)$$

$$b = \frac{E_{\mathrm{r}}}{RT(j-1)^2}(1 - a) \quad (38)$$

As the models are discretized in time and space, the relation of Δt and Δz has to hold to ensure solution stability and convergence of the discretization scheme. Penny and Lindfield suggest having the ratio of $D\Delta Z$ and Δt^2 not greater than 0.5.[13] The selection of Δz is based on the precision requirement for specific application. In this work, we choose Δz to be equal to 5 μm. The selection of Δt, however, is based on industrial control requirements (equal to 20 s in this work). These selections guarantee the solution stability and convergence. Usually, the smaller the Δz and Δt, the smaller the computational errors, but the bigger the memory usage. The applications shown in this work provide satisfactory computational precision.

Simulation Procedure

The state-space model in eqs 14−38 can be used for simulation by the following procedure.

Step 1. Input process and property data and model constants, such as $\mathcal{T}$, σ, h_{v}, ρ_{m}, $C_{\mathrm{p_m}}$, Z_{m}, Δt, ΔZ, E_{r}, E_{d}, R, L_i, γ, η, P_{sa}, and P_{a}, and calculate the number of time intervals needed for a vehicle to go through each zone, J_i, $i = 1, 2, \dots, N_z$ (the total number of zones), using eq 13.

Step 2. Input initial data of oven wall and convection air temperatures ($T_{\mathrm{w}}(0)$, $T_{\mathrm{a}}(0)$), air velocity (V_{a}) for each zone, vehicle initial temperature ($T(0)$), solvent distribution ($\mathbf{X}(0)$), film thickness ($Z(0)$), and diffusivity distribution ($\mathbf{D}(0)$).

Step 3. Calculate temperature $T(k+1)$ using eq 14. Note that if both radiation and convection are involved, coefficents a and b_1 need to be calculated using eqs 15a and 16a, otherwise using eqs 15b and 16b.

Step 4. Calculate diffusivity $D_n(j)$ using eq 33.

Step 5. Calculate solvent contents $\mathbf{X}(j+1)$ using eq 20.

Step 6. Calculate film thickness $Z(j+1)$ using eq 35.

Step 7. Calculate polymerization convection rate $x(j+1)$ using eq 36.

Step 8. Repeat the computations in steps 3−7 until the expected time steps (or the prediction horizon) are all calculated for all panels.

Note that, at a time interval Δt, the film thickness reduction, $(Z(j+1) - Z(j))$, is always less than Δz. After a number of time intervals, say $n\Delta t$, the accumulated thickness reduction will be equal to or just exceed Δz.

Table 1. Oven Temperature Settings

zone no.	heating mechanism	zone length (m)	radiation wall temp (K)	convection air temp (K)
1	IR/convection	20.73	473	403
2	IR/convection	13.41	478	478
3	convection	23.67		433
4	convection	23.67		428
5	convection	23.67		418
6	convection	10.54		418
7	air cooling	9.14		

At this time, the total number of slices of film will be reduced by 1, or the discretized thickness, $N\Delta z$, becomes $(N - 1)\Delta z$.

Case Study

A vehicle body consists of a number of panels, such as hood, roof, left and right outer front doors and sills, and lift gates.Because the heating environment in any zone of an oven is not completely uniformed, horizontal and vertical panels may have different heating histories. The temperature gradient among the panels may cause different drying rates and polymerization conversion rates. These are probably the main reasons for defect generation. The integrated model developed in this paper can be used to characterize the filmbuild of panels in the oven.

In this section, we conduct various simulations using industrial operational settings and constraints. It is intended to predict process behavior in an oven and to identify potential filmbuild problems. For those undesirable situations, we try to change relevant process parameters for improved process operation.

Process Specification. The operational settings of wall temperatures and convection air temperatures in a seven-zone oven are listed in Table 1. Vehicles on the conveyer move through the oven at the line speed of 0.069 m/s. It is assumed that the wet film on vehicles has the solvent content $\bar{X}(0)$ of 0.18 and the initial thickness of 70 μm. In operation, it is required that the temperature of any panel does not exceed 470 K. To have a desirable cross-linking structure of the dried film, the polymerization conversion rate should eventually be greater than 95% for any panel. To prevent defects caused by improper heating, the temperature increment cannot exceed 22.2 K/min, and the film drying rate, which is the rate of change of mean solvent residue in the film, must be below 0.0035 s^{-1}. For the dry film, the solvent content should be less than 0.03, and the film thickness needs to be in the range of 53.3 $\pm$ 5.1 μm.

For this case, the densities of the solid and solvent of paint are 1.2 and 1.0 g/cm^3, respectively. To simulate the process, the model constants γ, η, and ζ are set to 0.332, 9.38 $\times$ 10^{-6} m^2/s, and 5 $\times$ 10^{14} s^{-1}, respectively, and the activation energies for diffusion and reaction, E_d and E_r, are equal to 3.27 $\times$ 10^4 and 1.1 $\times$ 10^4 J/mol, respectively. The values of these constants γ, η, and E_d were obtained from the literature,[10] while the values of ζ and E_r were determined by the coating material we studied.

Model Prediction. Under the given operating conditions, the seven panels of a vehicle have different temperature distributions. Among them, the liftgate, named Panel 1, is found to have the hightest temperature, while the right outer front door, named Panel 2, has the lowest in all zones of the oven. Their temperature profiles are depicted by solid lines in Figure 4, where the symbols "*" and "◇" mark industrial data for different panels. Apperantly, the model predictions are very acceptable.

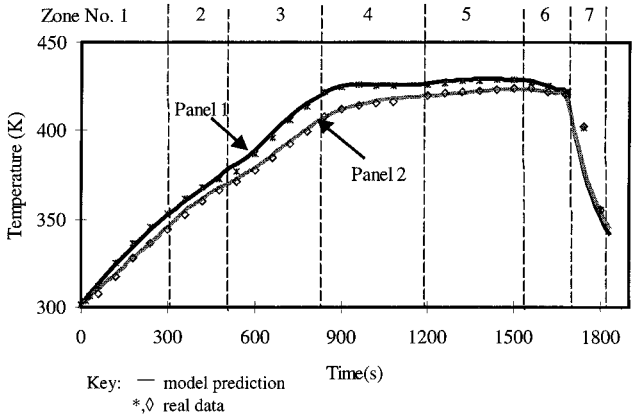

Figure 4. Temperature profiles of the two panels.

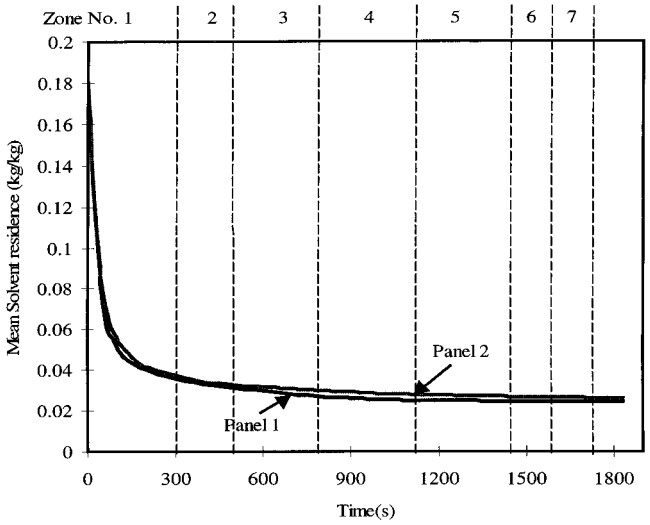

Figure 5. Solvent removal dynamics of the two panels.

We expect that the solvent in the film will be rapidly evaporated when the panels are heated. Figure 5 depicts the mean solvent removal dynamics. Note that most of the solvent is removed in the first two zones where both radiation and convection occur. The final solvent contents of the two panels are all below the specification (0.03 kg/kg). It seems that the temperature difference of the two panels shown in Figure 4 does not have any severe influence on solvent removal. The solvent removal dynamics of the panels are very close to each other. They should have nearly the same drying rates. The model simulation shows the agreement with the analysis. The drying rates of the two panels are very high during the first 30 s, but under the upper limit, they then fall down quickly in the following 4 min.

It is understandable that as the solvent is removed quickly, the film thickness is reduced accordingly. Figure 6 gives the film thickness changes of the two panels. It indicates that the panel temperature difference of about 10 K that existed in the first two zones does not make any noticeable difference for film thickness reduction. However, the panel temperature difference gives rise to quite different polymerization conversion rates (97.41% for Panel 1 and 87.39% for Panel 2), as shown in Figure 7. Clearly, the reaction conver-

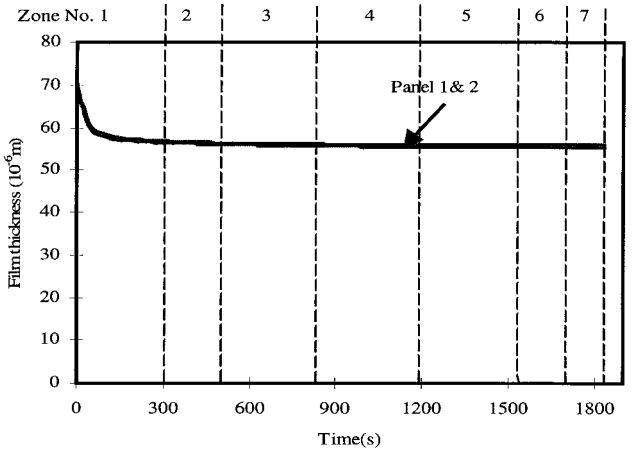

Figure 6. Film thickness change of the two panels.

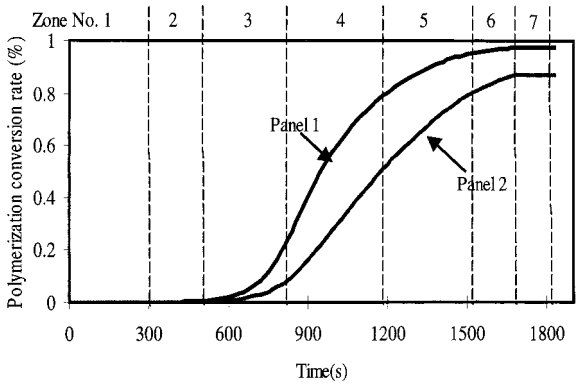

Figure 7. Polymerization conversion dynamics of the two panels.

sion of Panel 2 is incomplete; it is much lower than the requirement (95%).

Operational Improvement. The simulation results in Figures 4 and 7 indicate that the polymerization starts when the vehicle moves into the third zone (at the film temperature of about 390 K). It seems that if the temperature profile of Panel 2 in Zones 3−6 is very close to that of Panel 1, the conversion rate on Panel 2 will be improved dramatically. As shown in eqs 14, 15b, and 17, the panel temparature in those convection zones is determined by the convection air temperature, T_a, and the heat-transfer coefficient, h_v. According to eq 4, the heat-transfer coefficient is largely determined by the convection air velocity, V_a. Obviously, if we increase the convection air temperature, then all panel temperatures will be increased. Nevertheless, if we only increase the convection air velocity and/or flow rate in each relevant zone, then the heat-transfer coefficients will be different for those panels. Moreover, we can adjust the openness of the convection air nozzles near the particular panels of interest for the change of heat-transfer coefficients. All these allow us to reduce panel temperature differences. In this case, the heat-transfer coefficient is changed from 23 to 30 W/m^2·K. The new panel temperature profile is improved in Zones 3−5 and the polymerization conversion rate is correspondingly increased to 95.11%, as shown in Figure 8.

Process Analysis. The developed model can be used to conduct extensive simulation for revealing process dynamics under any initial wet coating condition and any operational mode. This will greatly help identify optimal operational strategies for the best filmbuild. For instance, if we assume that Panel 1 has different initial wet film thicknesses (70, 100, and 120 μm) in three

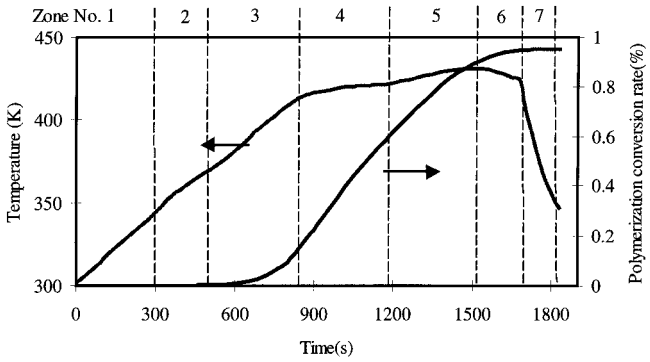

Figure 8. Improved temperature profile and polymerization conversion of Panel 2 after changing the convection air velocity in Zone 3.

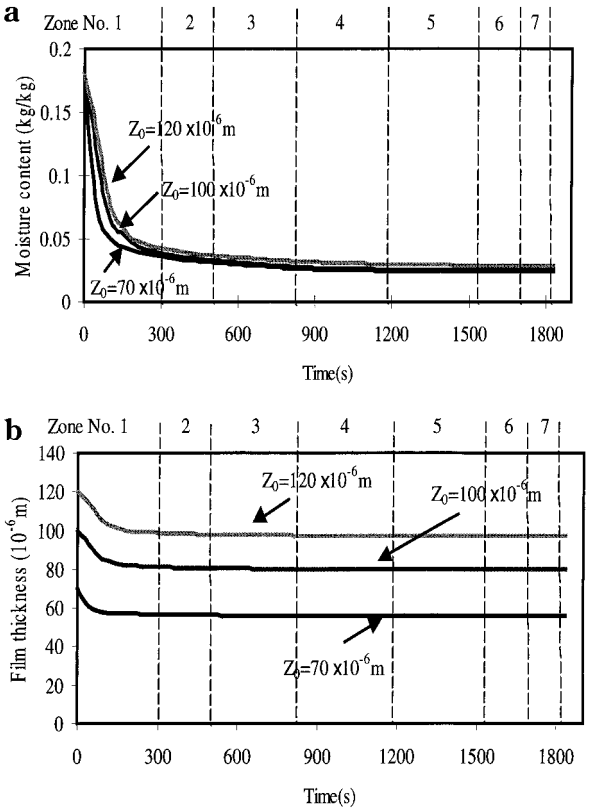

Figure 9. (a) Moisture content change in the three locations with different film thicknesses of a panel. (b) Film thickness dynamics for the three locations with different initial wet film thicknesses of a panel.

locations, then the model can depict solvent removal dynamics for the three cases. Figure 9a shows that the thinner film has faster reduction of moisture content than the thicker one. Correspondingly, the film thickness reductions in these three locations are also different, as illustrated in Figure 9b. In fact, the model can also be used to provide reversed predictions of process operations. For instance, if the dry film thickness of a panel is measured, we can run the model to calculate the wet film thickness when a vehicle moves into the oven.

The application study has indicated that a number of key parameters dominate the prediction of process dynamics. For instance, the reaction activation energy affects the cross-linking reaction most, and the drying operation in its early stage is very sensitive to the solvent partial pressure and mass-transfer coefficient, but the activation energy for diffusion becomes more

sensitive in later drying stages. These results are consistent with engineering judgment and are helpful for optimizing the reactive drying process.

Conclusion

Clearcoat drying and curing in an oven is a complicated reactive drying process. In this process, solvent removal and cross-linking reactions occur simultaneously, as vehicle bodies move continuously through the oven. In current practice, the oven operational settings are basically experience-based, and the oven feedback control is not based on vehicle condition, but on oven temperatures. To improve clearcoat filmbuild, it is crucial that the dynamics of the clearcoat film be revealed. This paper has introduced the first-principles-based, simplified, integrated plant floor models for predicting panel temperature profiles, solvent removal progress, film thickness changes, and cross-linking completeness in any zones of an oven at any time. The model has been partially validated using limited industrial data. If they are completely validated, the model can be used for reliable on-line monitoring of panel drying and curing operations. Initial model-based process analysis has demonstrated its great potential for optimizing process operation and improving coating quality.

Acknowledgment

This work is supported in part by the Institute of Manufacturing Research of Wayne State University.

Nomenclature

A = system matrix in the solvent drying model
B = control matrix in the solvent drying model
Bi = Biot number
C_p = heat capacity (J/kg·K)
D = diffusivity (m^2/s)
E_a = activation energy (J/mol)
h = heat-transfer coefficient (W/m^2·K)
j = discrete time instant
J = number of time intervals for a vehicle to go through an oven zone
k = thermal conductivity (W/m·K)
K = mass-transfer coefficient (kg/m^2·s)
l = metal substrate thickness (m)
L = zone length (m)
n = film slice index
N = number of film slices
P = pressure (Pa)
R = gas constant (8.314 Pa·m^3/mol·K)
R_{dry} = drying rate (s^{-1})
S = film surface area (m^2)
s = conveyer line speed (m/s)
t = time (s)
T = temperature (K)
U = control variable in the solvent drying model
x = monomer fractional conversion degree
X = solvent content in film (kg of solvent/kg of solid)
$\bar{X}$ = mean solvent content in film (kg of solvent/kg of solid)
X = vector of solvent content
v = volume (m^3)
V = velocity (m/s)
Z = thickness **(**m)
Δt = time interval (s)
ΔZ = film thickness of each slice (m)

Greek Letters

α = activity of solvent
β = constant
ξ = film thickness reduction during a time interval Δt
σ = Stefen−Boltzman constant (5.67×10^{-8} W/m^2·K^4)
$\mathcal{T}$ = viewing factor for radiation
ϵ = emissivity
ρ = density (kg/m^3)
κ = polymerization rate constant (1/s)
ζ = polymerization reaction frequency factor (1/s)
η = pre-exponential constant for diffusion (m^2/s)
γ = constant

Subscripts

a = convection air
c = clearcoat
d = diffusion
i = zone index
l = solvent in paint
m = metal substrate
n = film slice index
T = total heat transfer
v = convection
r = reaction
s = solids in paint
sa = saturation vapor of solvent
w = oven wall

Literature Cited

(1) Cohen, E. D.; Gutoff, E. B. *Modern Coating and Drying Technology*; VCH Publishers: New York, 1992.

(2) Gutoff, E. B.; Cohen, E. D. *Coating and Drying Defects*; John Wiley & Sons: New York, 1995.

(3) Marrion, A. R. *The Chemistry and Physics of Coating*; Royal Society Of Chemistry: Cambridge, U.K., 1994.

(4) Wu, S. M.; Ni, J.; Hu, S. Next Generation Quality Control in Manufacturing—Real Time Defect Prevention. *Proceedings of the ASME Winter Annual Meeting*, 1989.

(5) Blanc, D.; Vessort, S.; Laurfnt, P.; Gerard, J. F.; Andrieu J. Study and Modeling of Coated Car Painting Film by Infrared or Convective Drying. *Drying Technol.* **1997**, *15 (9)*, 2303.

(6) Dickie, R. A.; Bauer, D. R.; Ward, S. M.; Wagner, D. A. Modeling Paint and Adhesive Cure in Automotive Applications. *Prog. Org. Coatings* **1997**, *31*, 209.

(7) Howison, S. D.; Moriarty, J. A.; Ockendon, J. R.; Terrill, E. L.; Wilson, S. K. A Mathematical Model for Drying Paint Layers. *J. Eng. Math.* **1997**, *32*, 377.

(8) Koleske, J. V., Ed. *Paint and Coating Testing Manual*, 14th ed.; ASTM: Philadelphia, PA, 1995.

(9) Mccabe, W. L.; Smith, J. C.; Harriott, P. *Unit Operations Of Chemical Engineering*; McGraw-Hill Inc: New York, 1985.

(10) Navarri, P.; Andrieu, J. High-Intensity Infrared Drying Study. Part II. Case of Thin Coated Films. *Chem. Eng. Process.* **1993**, *32*, 319.

(11) Seborg, D. E.; Edgar, T. F.; Mellichamp, D. A. *Process Dynamics Control*; John Wiley & Sons: New York, 1989.

(12) Ogunnaike, B. A.; Ray, W. H. *Process Dynamics, Modeling, and Control*; Oxford University Press: Oxford, 1994.

(13) Penny, J.; Lindfield, G. *Numerical Methods Using Matlab*; Ellis Horwood: New York, 1997.

Received for review March 8, 1999
Revised manuscript received November 22, 1999
Accepted November 24, 1999

IE990171G